Spontaneous Thermocapillary Drops Interaction: The Effect of a Surface Reaction

L. Bialik-Rosenfeld, O. M. Lavrenteva, and A. Nir
Chemical Engineering Dept., Technion, Haifa 32000, Israel

DOI 10.1002/aic.11325
Published online October 1, 2007 in Wiley InterScience (www.interscience.wiley.com).

The spontaneous motion of small drops suspended in an immiscible viscous fluid, when an exothermal reaction occurs on their interfaces, has been studied. The heat of reaction results in an elevation of temperature on the drops' interfaces and in the external fluid. The concentration and temperature in the gap region become different from those in the outer regions. The inhomogeneous distribution of concentration and temperature induces surface tension variations, Marangoni type flow and migration of the fluid particles relative to each other. Cases studied concern two drops interaction due to thermocapillary forces induced by temperature field, the addition of a gravity field and the mutual effect of thermocapillary forces induced simultaneously by temperature and concentration. Results are presented for a variety of the governing parameters of the system. Stationary flow patterns with immobile drops configurations are predicted, which appear to be unstable for small perturbations. © 2007 American Institute of Chemical Engineers *AIChE J,* 53: 2783–2794, 2007
Keywords: fluid mechanics, heat transfer, mass transfer, transport

Introduction

Heat and mass transfer processes significantly influence the hydrodynamic interaction of drops and bubbles in nonisothermal multiphase systems. When a bubble or a drop is placed in a fluid in which the temperature or concentration of dissolved species change from one place to another, such variations can be expected at the interface. The consequence is a variation of the local tension on the surface. This variation causes a tangential surface traction from the lower tension region toward regions with higher interfacial tension, which results in motion on both sides of the interface and a net migration of the drop or the bubble toward the heat or species source may occurs. We refer to this motion, induced by either temperature or concentration gradients, as a thermocapillary or Marangoni migration.

Correspondence concerning this article should be addressed to A. Nir at avinir@techunix.technion.ac.il.

An early work describing thermocapillary migration that was induced by an external heat source was reported by Young et al.[1] They showed that bubbles could be held fixed against buoyant rise, and even move downward, by the application of a vertical temperature gradient. They also provided a theoretical description for the motion of a single bubble under conditions where inertial forces and convective transport of energy are negligible. Further theoretical treatments of the isolated bubble problem have been given by Bratukhin[2] who attempted to improve upon the solution of Young et al.[1] by a regular perturbation scheme in the Marangoni number, so as to include effects of inertia and shape deformation. In the following decades, extensive study of the thermocapillary migration of drops and bubbles was performed, stimulated by its importance for space applications. The results of Young et al.[1] were extended to the case of viscous drops, arbitrary external temperature field, thermocapillary migration in the presence of other neighboring inclusion, and external boundaries. The review article by Subramanian[3] and the book by Subramanian and Balasubramaniam[4]

contain comprehensive review of the available literature on the subject.

Levich[5] developed a consistent theoretical model describing Marangoni motion of drops and bubbles induced by the gradients of surfactants concentration. He showed that these gradients are not necessarily imposed externally, but they can appear locally, in a fluid, which has uniform concentration far from the drop, and can be brought about by the motion itself, thus displaying the feedback between the transport processes and hydrodynamics. LeVan and Newman[6] have studied the effect of dilute soluble surfactants on terminal velocity of the drop. In contrast to temperature, concentration of surfactants strongly affects not solely surface tension but also mobility and other rheological properties of the interface.

Davis and Acrivos[7] proposed a model for the creeping motion of a bubble contaminated by an "insoluble" surface-active agent, and Sadhal and Johnson[8] examined the creeping flow due to the motion of a liquid drop or a bubble in another immiscible fluid when the interface was partially covered by a stagnant layer of a surfactant. A stagnant layer model assumes that the interface becomes absolutely unmovable when the surfactant concentration reaches its saturation value, while for smaller concentration the mobility is not affected. Another popular model is a Newtonian interface introducing shear and dilatational surface viscosity. Marangoni migration of a drop with Newtonian interface was studied by LeVan.[9] A general model taking into account adsorption–desorption kinetics, surface diffusion, and convection of the surfactants can be found in Edwards et al.[10]

Ryazantsev[11] has shown that the nonuniformity of fluid flow around a chemically reacting droplet generates, due to convective effects, a nonuniform heat flux at the droplet interface. This induces surface tension gradients, which substantially affect the drag force acting on the droplet. The effect of convection can be significantly strong and lead to the appearance of a traction force and to a spontaneous drift of the droplet even against body forces. This work is another demonstration of selfinduced surface tension gradients.

Surface tension gradients causing motion of drops and bubbles can also appear in the course of interphase mass and heat transfer as a result of a geometric nonuniformity of the system. For instance, when two adjacent drops are not in thermal equilibrium with the fluid in which they are suspended heat is transferred across the interfaces into the bulk and the process results in an elevation of the temperature in the gap between the two drops. Since the temperature in the gap between the drops is higher than in other regions on the drops surfaces, the surface tension there is lowered. The resulting surface tension gradients induce a motion of the surrounding fluid out of the gap, thus forcing the drops to approach each other. When the transfer of heat or mass is from the continuous phase into the dispersed one, the surface tension gradients are directed oppositely, which lead to a repulsion of the droplets. This mechanism was first suggested and studied by Golovin et al.[12] Golovin[13] demonstrated that similar interaction induces a thermocapillary migration of solid particle. The results of further investigation of the spontaneous thermocapillary interaction of bubbles and drops are summarized in Lavrenteva et al.[14]

A celebrated method of solving problems involving two spherical fluid particles is to express the relevant flow and conservation fields via the use of bispherical coordinate system. One of the early such works describing the slow viscous hydrodynamic interaction between two spherical solid particles was reported by Stimson and Jeffery.[15] This study was generalized by Haber et al.,[16] who studied the velocity fields for two drops. Other studies on the interactions between two spherical drops or bubbles, or among a chain of spherical drops or bubbles, undergoing thermocapillary migration were performed by Meyyappan et al.,[17] Meyyappan and Subramanian,[18] and Keh and Chen.[19]

When the nonuniform temperature or concentration distributions are caused by a nonisothermal chemical reaction on the surface of the bubble or drop, the appearance of the temperature gradients and the thermocapillary traction associated with it are expected to be a consequence of both the reactants concentration and the reaction temperature distributions. The chemical reaction can cause a combined effect of nonuniform temperature and concentration distributions, which will affect simultaneously the driving force for drop migration. These forces can work with or against each other and thus can cause different motion patterns. This subject, as well as the dynamic interaction of two drops due to chemical reaction has not yet been thoroughly investigated.

The goal of the present work is to study the dynamic interaction of two drops at an arbitrary nonzero separation distance due to an exothermic chemical reaction, which takes place on their surfaces. We note parenthetically that the approach taken is this article applies equally to an endothermic surface reaction, however, with an induced reverse dynamics. We begin by studying the spontaneous motion of two drops in the absence of the gravity force. The driving force for the motion of the drops is a surface tension gradient, which is created solely by the temperature gradient, an outcome of the reaction rate that occurs on the surface. We further consider the simultaneous effect of this thermocapillary force and gravity field. Finally, the simultaneous effect of reaction temperature and concentration of the reactants on the driving force and the resulting flow patterns is examined.

Problem Formulation

Assume a system containing two drops of equal size and of the same material submerged in an immiscible unbounded fluid which is quiescent and has a uniform constant temperature, $\hat{T}_\infty$, and a uniform constant solute concentration of species A, $\hat{C}_\infty$, at infinity. Species A approaches each of the drops surfaces by diffusion and reacts with species B, which reaches the surface from inside the drops.

The chemical reaction is of the form A + B $\rightarrow$ C. It is assumed to be exothermic and its rate is proportional to the concentration of each reactant. Because of the interaction between the drops, the concentration of species A on the surface of each one is not uniform. This generates a nonuniform reaction rate and, thus, a temperature gradient appears on the surface of the drops. This gradient becomes the driving force for the motion of the drops relative to each other since it creates a surface tension gradient on the interfaces.

We assume that the cores of the drops have the same concentration of species B and that the latter does not change

significantly during the characteristic time of the drops' motion. The diffusion coefficient inside the drops is assumed to be large so that the concentration there is uniform and B is immediately available to the surface. Under these assumptions the reaction can be considered as a first order reaction with $\hat{C}$ referring to the concentration of species A. We further assume that species C, produced by the reaction, migrates instantaneously from the surface and does not affect surface properties.

The basic equations that describe the problem include the dynamic heat and mass balances for the transport of heat and mass inside the drops and in the surrounding domain and momentum balances for the Newtonian fluids.

It is supposed further that the concentration and temperature do not affect any physical properties of the liquids in the bulk and at the interfaces except for the interfacial tension which is considered to depend linearly on the temperature, $\hat{\gamma} = \hat{\gamma}_0 + \frac{\partial \hat{\gamma}}{\partial \hat{T}}\left(\hat{T} - \hat{T}_\infty\right)$. In the last section the interfacial tension is assumed to depend simultaneously on the temperature and the concentration of species A, $\hat{\gamma} = \hat{\gamma}_0 \left(1 + \frac{\partial \hat{\gamma}}{\partial \hat{T}}\left(\hat{T} - \hat{T}_\infty\right)\right)\left(1 + \frac{\partial \hat{\gamma}}{\partial \hat{C}}\left(\hat{C} - \hat{C}_\infty\right)\right)$, where $\frac{\partial \hat{\gamma}}{\partial \hat{T}}$ and $\frac{\partial \hat{\gamma}}{\partial \hat{C}}$ are constant and typically negative. In what follows, the index $i = 1$ and 2 distinguishes between the drops and the ambient fluid. Thus, Ω_1 and Ω_2 are the domains occupied by the dispersed and continuous phases, respectively.

The system is rendered nondimensional by using the following typical dimensions: $\hat{a}$ for length, $\hat{U} = \left|\frac{\partial \hat{\gamma}}{\partial \hat{T}}\right| \frac{\hat{T}_\infty}{\hat{\mu}_2}$ for velocity, $\hat{T}_\infty$ for temperature, $\hat{C}_\infty$ for concentration, $\frac{\hat{\mu}_2 \hat{U}}{\hat{a}}$ for pressure, $\hat{\gamma}_0$ for surface tension, and $\frac{\hat{a}}{\hat{U}}$ for the time. Here $\hat{a}$ is the drop radius, $\hat{T}_\infty$ and $\hat{C}_\infty$ are the temperature and concentration of species A at infinity and $\hat{\mu}_i\,(i = 1, 2)$ denote the viscosity of the inner and outer fluids, respectively.

We suppose that the reference interfacial tension corresponding to the temperature and concentration far away from the drops, $\hat{\gamma}_0$, is sufficiently large to preserve the spherical shape of the drops. We further suppose that, at any moment, the motion is sufficiently slow, inertia effects are negligible, and the Stokes-approximation holds. The velocities of the drops, as yet unknown, should be found from the condition that the total force acting on each drop is zero. It is assumed that both Péclet numbers in terms of mass and heat transfer ($Pe_T^i = \frac{\hat{a}\cdot\hat{U}}{\hat{\chi}_i}$, $Pe_C = \frac{\hat{a}\cdot\hat{U}}{\hat{D}}$, where $\hat{D}$ and $\hat{\alpha}_i$ denote diffusivity and thermal diffusivity in the phase i, respectively) are zero, which means that diffusion and conduction are the governing transport mechanisms while convective effects are negligible. These assumptions bring forward the analyzed effect, i.e. the induction of drop dynamics by the presence of surface chemical reaction, yet help reducing the number of physical parameters without altering the phenomenon qualitatively.

Under the assumptions that were described above we obtain the following dimensionless system of equations describing the problem:

$$\nabla^2 C = 0, \quad \mathbf{x} \in \Omega_2, \tag{1}$$

while for $i = 1, 2$

$$\nabla^2 T_i = 0, \quad \mathbf{x} \in \Omega_i, \tag{2}$$

$$\mu_i \nabla^2 \mathbf{v}_i - \nabla P_i = 0, \quad \mathbf{x} \in \Omega_i, \tag{3}$$

$$\nabla \cdot \mathbf{v}_i = 0, \quad \mathbf{x} \in \Omega_i. \tag{4}$$

Here $\mu_i = \frac{\hat{\mu}_i}{\hat{\mu}_2}$ with $\mu_2 = 1$ and $\mu_1 = \lambda$.

Notice that in the absence of inertia and convective transport the equations become linear and can be solved analytically. Moreover, the heat and mass balances and the momentum equations are partly decoupled. The concentration can be determined for each configuration independently from the temperature and velocity fields. Nevertheless, the coupling of the system is retained via the heat production by surface chemical reaction as well as via the dependence of the interfacial tension on the temperature and concentration of species A. Moreover, a complicated dependence of the induced velocities on the geometry (separation between the drops) preserves the nonlinear nature of the dynamics of the interacting drops.

The appropriate boundary conditions are of the form:

$$\nabla C \cdot \mathbf{n} = \phi^2 C, \quad \mathbf{x} \in \Gamma, \tag{5}$$

where Γ denotes the interface between two phases and ϕ stands for Thiele modulus $\left(\phi = \hat{a}\sqrt{\frac{\hat{k}}{\hat{D}}}\right)$.

$$C = 1, \quad |\mathbf{x}| \to \infty. \tag{6}$$

$$L_B C = \nabla T_1 \cdot \mathbf{n} - \kappa \nabla T_2 \cdot \mathbf{n}, \quad \mathbf{x} \in \Gamma, \tag{7}$$

where $L_B = \frac{\hat{\lambda}^* \hat{k} \hat{C}_\infty}{\hat{\kappa}_1 \hat{T}_\infty}$ and $\kappa = \frac{\hat{\kappa}_2}{\hat{\kappa}_1}$. Here, $\hat{\kappa}_1$ and $\hat{\kappa}_2$ are the thermal conductivities of the inner and outer fluids respectively, $\hat{k}$ is the reaction rate, $\hat{\lambda}^*$ is the latent heat of the reaction and $\mathbf{n}$ is a unit vector normal to the drop surface pointing outward.

$$T_1 = T_2\ , \quad \mathbf{x} \in \Gamma, \tag{8}$$

$$T_2 \to 1 \quad |\mathbf{x}| \to \infty, \tag{9}$$

$$T_1 \text{ is finite everywhere}, \tag{10}$$

$$\mathbf{v}_1 = \mathbf{v}_2, \ \mathbf{x} \in \Gamma, \tag{11}$$

$$\mathbf{n} \cdot (\boldsymbol{\sigma}_2 - \boldsymbol{\sigma}_1) \cdot \boldsymbol{\tau} = \frac{\partial \gamma}{\partial \boldsymbol{\tau}}, \quad \mathbf{x} \in \Gamma, \tag{12}$$

where $\boldsymbol{\tau}$ is a unit vector tangential to the surface, $\boldsymbol{\sigma}_1$, $\boldsymbol{\sigma}_2$ are the inner and outer stress tensors, respectively.

Methods of Solution

A natural description choice for the system of two nontouching spherical bodies is the three dimensional bispherical coordinate system (α, β, and φ) conjugate to the cylindrical coordinates ρ, z and φ (see Figure 1), defined by the mapping $z + i\rho = ic\cot\frac{\alpha + i\beta}{2}$ or $\rho = \frac{c\sin\alpha}{\cosh\beta - \cos\alpha}$, $z = \frac{c\sinh\beta}{\cosh\beta - \cos\alpha}$, where $2c$ denotes the distance between the poles (see e.g. Lebedev[20]). For equal size drops, the interface of the leading droplet on the right is described by the coordinate surface $\beta = \beta_0 > 0$ and the interface of the second trailing droplet corresponds to $\beta = -\beta_0 < 0$. The drop's dimensionless radius is given by $\frac{c}{\sinh\beta_0}$. Since the normalized radius is equal to 1, we have $c = \sinh\beta_0$ and the separation distance between the drops is $d = 2(\cosh\beta_0 - 1)$.

In this coordinate system, the Laplace equation has the form[20]:

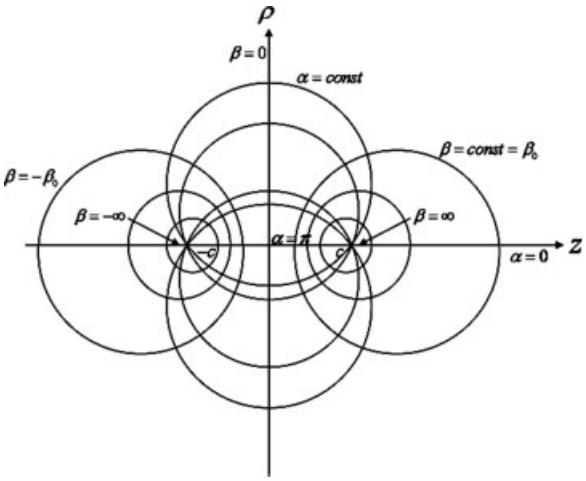

Figure 1. Bispherical coordinate system connected with the pair of drops.

$$\frac{\partial}{\partial\alpha}\left(\frac{\sin\alpha}{\cosh\beta-\cos\alpha}\frac{\partial C}{\partial\alpha}\right)+\frac{\partial}{\partial\beta}\left(\frac{\sin\alpha}{\cosh\beta-\cos\alpha}\frac{\partial C}{\partial\beta}\right)+\frac{1}{(\cosh\beta-\cos\alpha)\sin\alpha}\frac{\partial^2 C}{\partial\varphi^2}=0.$$

In view of the axial symmetry of the problem and the lack of dependence on φ, the $\frac{\partial^2 C}{\partial\varphi^2}$ term is set to zero.

The general solutions for the concentration and temperature profiles are given by (see, e.g. Lebedev[20]):

$$C=1+(\cosh\beta-\eta)^{1/2}\sum_{n=0}^{\infty}U_n(\beta)\,P_n(\eta), \tag{13}$$

$$T_1=(\cosh\beta-\eta)^{1/2}\sum_{n=0}^{\infty}V_n^{(\pm1)}(\beta)P_n(\eta), \tag{14}$$

and

$$T_2=1+(\cosh\beta-\eta)^{1/2}\sum_{n=0}^{\infty}V_n^{(2)}(\beta)P_n(\eta). \tag{15}$$

In the above expressions $P_n(\eta)$ are Legendre polynomials and $\eta=\cos\alpha$, while the functions U_n, $V_n^{(\pm1,2)}$ are of the form:

$$U_n=H_n\cosh\left(\left(n+\frac{1}{2}\right)\beta\right)+I_n\sinh\left(\left(n+\frac{1}{2}\right)\beta\right),$$

$$V_n^{(\pm1)}=D_n^{\pm}\cosh\left(\left(n+\frac{1}{2}\right)\beta\right)+E_n^{\pm}\sinh\left(\left(n+\frac{1}{2}\right)\beta\right),$$

and

$$V_n^{(2)}=F_n\cosh\left(\left(n+\frac{1}{2}\right)\beta\right)+G_n\sinh\left(\left(n+\frac{1}{2}\right)\beta\right),$$

where the latter two correspond to the inner and outer temperature distributions, and the superscripts ±1 correspond to the leading and trailing drops, respectively.

The expressions (13) and (15) satisfy the boundary conditions at infinity (boundary conditions (6) and (9)). Substituting the solutions for the concentration and for the temperature into the appropriate boundary conditions ((5) for the concentration and (7), (8) for the temperatures) we arrive at the infinite systems of linear equations for the coefficients H_n, D_n, and F_n:

$$e_{-1}^n H_{n-1}-e_0^n H_n+e_{+1}^n H_{n+1}=\phi^2\sqrt{2}\exp\left[-\left(n+\frac{1}{2}\right)\beta_0\right], \tag{16}$$

$$-g_{-1}^n\cdot D_{n-1}+g_0^n\cdot D_n-g_{+1}^n D_n = u^n+L_B H_n\cosh\left(\left(n+\frac{1}{2}\right)\beta_0\right) \tag{17a}$$

$$F_n=\frac{\left(D_n-\sqrt{2}\right)\exp\left(-\left(n+\frac{1}{2}\right)\beta_0\right)}{\cosh\left(\left(n+\frac{1}{2}\right)\beta_0\right)}. \tag{17b}$$

Note that, due to the fore-and-aft symmetry of the problem we obtain that $D_n^+=D_n^-=D_n$ and $I_n=G_n=0$ for all n, while, from the requirement (10), it follows that $D_n^{\pm}\pm E_n^{\pm}=0$. The coefficients $e_{\pm1,0}^n$, $g_{\pm1,0}^n$ and u^n are given in the Appendix.

The system (16) and (17) is solved as proposed by Meyyappan et al.[17,18] and Keh and Chen.[19] It is truncated and solved repeatedly to ensure convergence within a given degree of accuracy. The size of the remaining series depends on the desired accuracy and on the separation distance between the drops.

In the bispherical coordinate system, the axi-symmetric flow fields in the continuous fluid and inside the drops are described by the dimensionless Stokes equations:

$$E^2\left(E^2\psi^{(\pm1,2)}\right)=0. \tag{18}$$

with $E^2=h\left[\frac{\partial}{\partial\beta}\left(h\frac{\partial}{\partial\beta}\right)+(1-\mu^2)\frac{\partial}{\partial\mu}\left(h\frac{\partial}{\partial\mu}\right)\right]$.

Here, the stream function ψ is described by: $u_\beta=\frac{h}{\rho}\frac{\partial\psi}{\partial\alpha}$, $u_\alpha=-\frac{h}{\rho}\frac{\partial\psi}{\partial\beta}$ and the metric coefficient, $h=\frac{\cosh\beta-\cos\alpha}{c}$. There should be no fluid flow at infinity and the velocities of the fluid inside the drops should be bounded, hence, $\frac{\psi^{(2)}}{\rho^2}=0$ @ $\beta=0,\ \alpha=0$ and $\frac{\psi^{(\pm1)}}{\rho^2}<\infty$

The continuity of surface velocity obtains the forms:

$$\psi^{(\pm1)}=\psi^{(2)},\quad \beta=\pm\beta_0, \tag{19a}$$

$$\frac{\partial\psi^{(\pm1)}}{\partial\beta}=\frac{\partial\psi^{(2)}}{\partial\beta},\quad \beta=\pm\beta_0, \tag{19b}$$

while the values of the streamfunction on the undeformable interfaces become

$$\psi^{(2)}=\frac{-V^{(\beta_0,-\beta_0)}\sin^2\alpha}{2h^2}. \tag{19c}$$

Here $V^{(\beta_0,-\beta_0)}$ are yet unknown projections of the dimensionless velocity of the drops on the z-axis.

The remaining boundary condition, which links the temperature and the velocity fields, is the balance of the tangential stresses at the interfaces of the drops (Eq. 12).

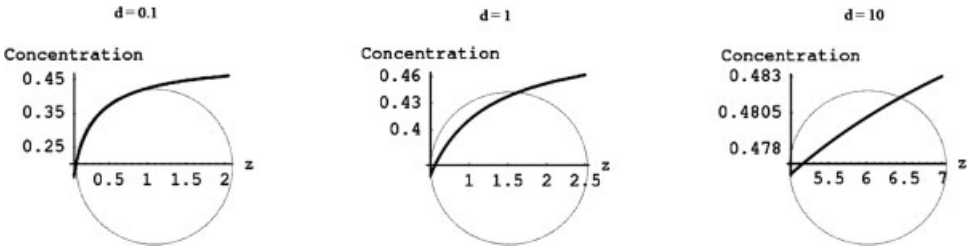

Figure 2. Concentration profiles on the surface of the right drop for various distances between the drops' surfaces, d: $\phi^2 = 1, \kappa = 1, L_B = 1$.

This balance, in bispherical coordinate system, gives:

$$\sigma_{\beta\alpha}^{(2)} - \sigma_{\beta\alpha}^{(\pm 1)} = \pm h \frac{\partial \gamma}{\partial \alpha}, \quad \beta = \pm \beta_0, \tag{20}$$

where $\sigma_{\beta\alpha}$ is the tangential component of the viscous stress tensor

$$\sigma_{\beta\alpha} = \mu \left[h \left(\frac{\partial u_\beta}{\partial \alpha} + \frac{\partial u_\alpha}{\partial \beta} \right) + \frac{1}{c} \left(u_\alpha \sinh \beta + u_\beta \sin \alpha \right) \right].$$

The general solution for Eqs. 18a,b was found by Stimson and Jeffery[15]:

$$\psi^{(i)} = (\cosh \beta - \eta)^{-3/2} \sum_{n=1}^{\infty} W_n^{(i)}(\beta)\, C_{n+1}^{-1/2}(\eta), \quad i = \pm 1,\ 2. \tag{21}$$

Where, $C_{n+1}^{-1/2}(\mu)$ are the Gegenbauer polynomials of order $n + 1$ and degree $-1/2$. In (21)

$$W_n^{(\pm 1,2)} = J_n^{(\pm 1,2)} \cosh\left(\left(n - \frac{1}{2} \right) \beta \right) + K_n^{(\pm 1,2)} \sinh\left(\left(n - \frac{1}{2} \right) \beta \right) + L_n^{(\pm 1,2)} \cosh\left(\left(n + \frac{3}{2} \right) \beta \right) + M_n^{(\pm 1,2)} \sinh\left(\left(n + \frac{3}{2} \right) \beta \right),$$

Combining expressions (19), (20), and (21) we obtain:

$$\sum_{n=1}^{\infty} \left(\frac{d^2 W_n^{(2)}}{d\beta^2} - \lambda \frac{d^2 W_n^{(\pm 1)}}{d\beta^2} \right) C_{n+1}^{-1/2}(\eta) = \pm \frac{c^2 (1 - \eta^2)}{(\cosh \beta - \eta)^{1/2}} \frac{\partial T}{\partial \eta} + (1 - \lambda) V^{(\pm \beta_0)} c^2 \left(1 - \eta^2 \right) \left(-\frac{3}{8} \frac{\sinh^2 \beta}{(\cosh \beta - \eta)^{5/2}} + \frac{1}{4} \frac{\cosh \beta}{(\cosh \beta - \eta)^{3/2}} \right). \tag{22}$$

The motion of the drops is the outcome of two opposite forces acting on each droplet. The Marangoni force, the first term on the right hand side of Eq. 22, is the result of the temperature gradient on the surface of each drop, which causes a surface tension gradient. This surface tension gradient causes the drift of the drops toward each other. The second force, resulting from the second term on the right hand side of (22), which works against the Marangoni force, is the Stokes resistance.

Under the quasi equilibrium assumption, the summation of the two forces should be zero so that the total force acting on each drop vanishes.

This force is being calculated following the expression derived by Stimson and Jeffery[15]:

$$F^{(\pm \beta_0)} = \frac{2\sqrt{2}\,\pi}{c} \sum_{n=1}^{\infty} \left(J_n^{(2)} \pm K_n^{(2)} + L_n^{(2)} \pm M_n^{(2)} \right) = 0 \tag{23}$$

We further examine the combined effect of gravity and thermocapillarity. To find the drops velocities, one has to modify the conditions (23) and equate the new viscous forces acting on the drops to the mass forces. Golovin et al.[12] have suggested different scaling for the velocity in this case, namely, the characteristic velocity of the drop motion driven by buoyancy: $\frac{\Delta\hat{\rho}\hat{g}\hat{a}^2}{\hat{\mu}^{(2)}}$, where $\Delta\hat{\rho}$ is the density difference between the drops and the continuous phase and $\hat{g}$ is the acceleration of gravity. In this case, Eq. 22 becomes:

$$\sum_{n=1}^{\infty} \left(\frac{d^2 W_n^{(2)}}{d\beta^2} - \lambda \frac{d^2 W_n^{(\beta_0, -\beta_0)}}{d\beta^2} \right) C_{n+1}^{-1/2}(\mu) = \pm \frac{c^2 (1 - \eta^2)}{(\cosh \beta - \eta)^{1/2}} m \frac{\partial T}{\partial \eta} + (1 - \lambda) V^{(\beta_0, -\beta_0)} c^2 \left(1 - \eta^2 \right) \left(-\frac{3}{8} \frac{\sinh^2 \beta}{(\cosh \beta - \eta)^{5/2}} + \frac{1}{4} \frac{\cosh \beta}{(\cosh \beta - \eta)^{3/2}} \right). \tag{24}$$

where, $m = \frac{-\frac{\partial \hat{\gamma}}{\partial \hat{T}} \hat{T}_\infty}{\Delta\hat{\rho}\hat{g}\hat{a}^2} = \frac{Ma_1}{(Ar)(Sc)}$ is the parameter characterizing the influence of the surface tension forces on the gravity-induced motion; $Ma_1 = \frac{-\hat{a}\frac{\partial \hat{\gamma}}{\partial \hat{T}} \hat{T}_\infty}{\hat{\mu}^{(2)} \hat{D}}$ is a modified Marangoni number, associated with surface tension gradients resulting from temperature variations rather than concentration changes, $Ar = \frac{\Delta\hat{\rho}\hat{g}\hat{a}^3}{\hat{\mu}^{(2)}\hat{\nu}}$ is the Archimedean number, and $Ac = \frac{\hat{\nu}}{\hat{D}}$ is the Schmidt number. Note that in most cases involving heavy drops, for which $\Delta\hat{\rho} > 0$, m, and Ma_1 obtain positive values since for most materials $\frac{\partial \hat{\gamma}}{\partial \hat{T}}$ is negative.

Results and Discussion

Motion of two equal drops due to the effect of a temperature gradient induced by a surface exothermic reaction

The concentration and temperature profiles on the surfaces of the drops in the case of a surface exothermic chemical reaction (calculated using Eqs. 13–15 with the coefficients given in (17), (18)) are presented in Figures 2 and 3. Because of the for-and-aft symmetry with respect to the plane $z = 0$ these profiles are depicted on the surface of the leading drop only. It can be seen that, when the distance between the drops is small, the concentration and temperature profiles

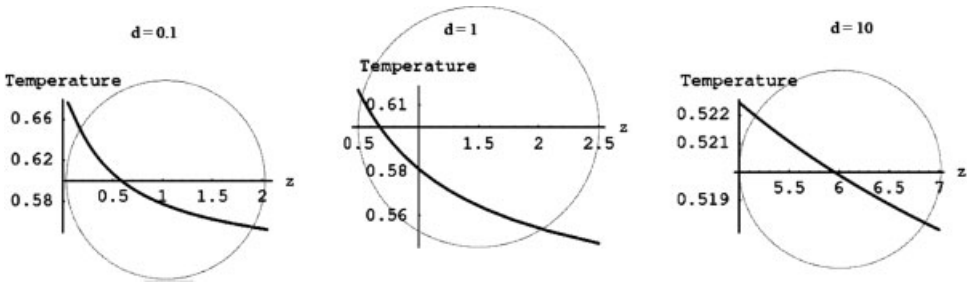

Figure 3. The influence of the distance, d, between the drops surfaces on the interfacial temperature profile of the right drop: $\phi^2 = 1,\ \kappa = 1, L_B = 1$.

obtain considerable gradients on the surface of each drop. When the distance between the drops becomes larger, the mutual effect of the drops diminishes and the distributions of concentration and temperature on the surface of the drops become similar to those observed on a single isolated drop.

The lower value of the concentration is located in the gap between the drops since the rate of diffusion of species A to the gap is slower than to other regions on the surface and hence the reaction rate in that region is slower than in other regions. Despite of this lower production of heat in the gap, for this choice of parameters, the temperature has the opposite tendency; the higher value is located in the gap between the drops since the removal of heat in that area is poor compared to that at the rest of the drop surface.

Iso-concentration and iso-temperature contours are presented in Figures 4 and 5. Both figures show closed contours around each drop that spread out when the distance is very small. The figures emphasize again the difference between large and small separation distances between the drops. While for large separation distance the concentration and temperature on the surface of each drop are almost constant and, hence, the reaction rate and temperature are almost uniform, noticeable variations in the concentration and temperature profiles appear when the separation distance is smaller. Figure 5 reveals also the change of temperature inside the drops.

The model and calculations predict that the main result of the nonuniform temperature distribution is manifested in the drops approaching each other. Figure 6 shows the influence of the different parameters of the system on the approach velocity of the upper drop. All four figures show a similar tendency, where the velocity increases to a maximum value at an "optimal" separation distance, which is a function of the governing parameters. For large separation distances the velocity decreases to zero since the mutual effect of the drops vanishes and there are no surface tension gradients and thus no driving force for the motion. For distances that are shorter than the optimal separation distance the viscous resistance to the motion induced by the Marangoni forces increases and this results in a velocity decrease.

In Figure 6a the dependence of the approach velocity on the viscosity ratio between the inner and outer fluids ($\lambda = \frac{\mu_1}{\mu_2}$) is presented. For small values of λ, the viscosity of the outer fluid is higher than the viscosity of the inner fluid and hence the fluid particle is closer to a bubble. In this case the loss of energy is smaller and we observe higher velocity than for cases with larger λ values. When λ has high values, the viscosity of the outer fluid is lower and the fluid particle resembles a rigid sphere. In this case the energy lost inside the drop is important and we observe smaller velocity values. The effect of Thiele modulus on the velocity of the drops (Figure 6b) shows that for small values of Thiele modulus (smaller than $O(1)$), the diffusion rate of species A to the surface is relatively high and thus more heat is produced in the gap between the drops which results in high temperatures and temperature variations on the surfaces of the drops and higher value of the velocity. For higher Thiele modulus values, the diffusion rate decreases and the total effect considerably diminishes.

The parameter L_B represents the ratio between the heat production rate and the rate of heat transfer by conduction inside the drops. Its influence on the drop velocity is given in Figure 6c. For small values of L_B, the heat production is low or the heat transfer is relatively high, which results in almost uniform low temperature on the surface and hence the approach velocity of the drops is very low. For higher L_B

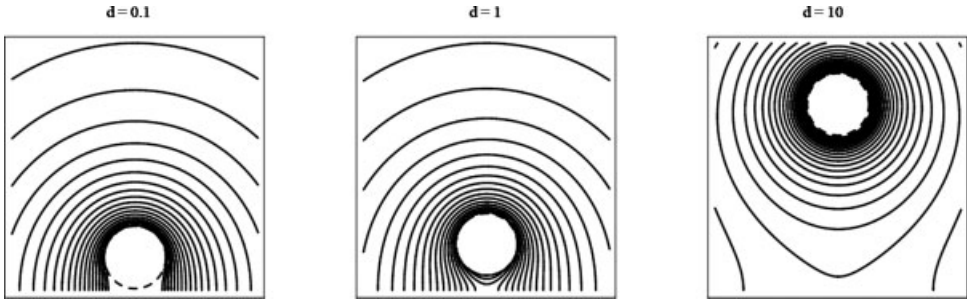

Figure 4. Iso-concentration lines of the concentration field around the upper drop for various distances between the drops: $\phi^2 = 1, \kappa = 1, L_B = 1$.

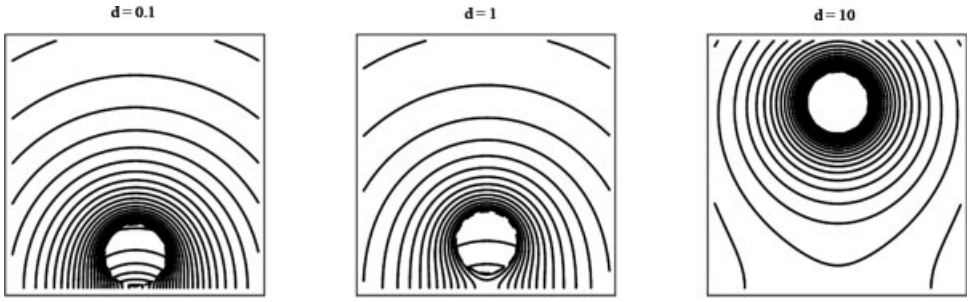

Figure 5. Iso-temperature lines for the temperature field around and inside the upper drop for various distances between the drops: $\phi^2 = 1$, $\kappa = 1, L_B = 1$.

values, the heat production is augmented, the temperature variation on the surface increases and the velocity of the drops attain higher values. The effect of the inner and outer thermal conductivity ratio ($\kappa = \frac{\kappa_2}{\kappa_1}$ in Figure 6d) is similar to the effect of the L_B parameter.

In Figure 7 we depict the dependence of the optimal separation distance (the separation distance in which the velocity of the drops obtains its maximum value) on the different parameters of the system. The curves in Figure 7 are calculated for all parameters but one equal to unity. It can be seen that for all the parameters the value of the optimal separation distance increases as the value of the parameter increases.

Golovin et al.[12] have showed that in the case of a surface tension gradient which is the outcome of a concentration variation on the surface of the drop that results from a cross surface transport, the maximum approach velocity value at separation distance of 0.3 is ~ 0.012 for the case $\lambda = 1$. These values agree well with the range of our results shown in Figures 6 and 7 in spite of the different process causing the gradients on the surface, i.e. a surface reaction resulting from diffusion to the surface.

Flow pattern (streamlines) for the system of the two drops is presented in Figure 8. As expected, the drops approach each other when the heat transfer is the outcome of the exothermic reaction.

It is interesting to examine the relevance of the above results to practical systems. We next consider a physical two-phase system by estimating the approach velocity of the spontaneous motion of two drops of aqueous solution of the viscosity $\hat{\mu}_1 = 1.002 \cdot 10^{-3} \frac{N \cdot sec}{m^2}$ that are suspended in silicone oil of the viscosity $\hat{\mu}_2 = 0.102 \frac{N \cdot sec}{m^2}$. Consider two drops having 1-mm radius each and 1-mm separation distance. Suppose that the drops undergo an exothermal chemical reaction of the first order in which the latent heat is, say, $1.4644 \cdot 10^8 \frac{J}{Kgmol}$ and the reaction rate coefficient is $\hat{k} = 0.1254 \frac{1}{sec}$. We let $\frac{\partial \hat{\gamma}}{\partial T}$ be $-1.87 \cdot 10^{-4} \frac{N}{m^{.0}C}$, the diffusion coefficient of small molecular solutes in the outer fluid be $D = 5 \cdot 10^{-9} \frac{m^2}{sec}$, and the thermal diffusivities of the outer and inner fluids be estimated by $\hat{\alpha}_1 = 2.351 \cdot 10^{-7} \frac{m^2}{sec}$ and $\hat{\alpha}_2 = 1.4376 \cdot 10^{-7} \frac{m^2}{sec}$, respectively. Under these conditions we obtain that the migration velocity equals $1.867\ 10^{-5} \frac{m}{sec}$. With this speed, the Péclet numbers in this case become $Pe_T = 1.33 \cdot 10^{-3}$, $Pe_C = 0.03734$, the Reynolds number becomes $\mathrm{Re} = 1.86164 \cdot 10^{-7}$, all indeed small and justifying the assumption of negligible inertia and convective effects,

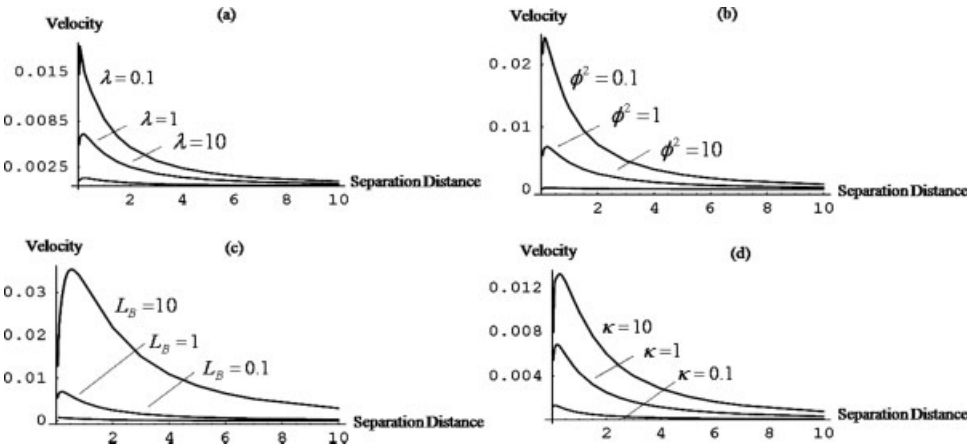

Figure 6. The dependence of the velocity of the upper drop on the separation distance for different parameters of the system.

(a) Various viscosity ratios, λ; $\phi^2 = 1$, $\kappa = 1$, $L_B = 1$; (b) Various Thiele modulus values, ϕ^2; $\kappa = 1, L_B = 1, \lambda = 1$; (c) Various L_B values, $\lambda = 1$, $\phi^2 = 1$, $\kappa = 1$. (d) Various thermal conductivity ratios, κ; $L_B = 1, \phi^2 = 1$, $\lambda = 1$.

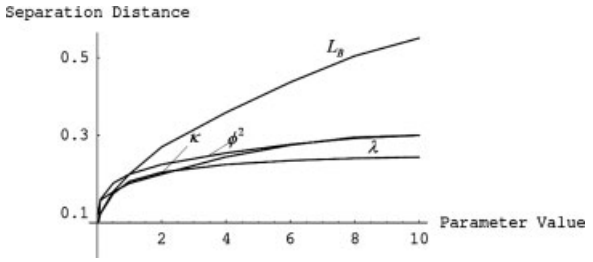

Figure 7. The dependence of the separation distance at which the approach velocity is maximum on the values of the different parameters of the system.

For each curve, all fixed parameters equal unity.

and the parameters L_B and ϕ^2 are $L_B = 4.095$, $\phi^2 = 4.472$. These estimates show that the effect of the surface reaction on the motion of the two drops is significant and that the assumptions made in our model were physically sound.

The influence of the gravity field on the motion of the drops

In this section we assess the mutual interaction of the thermocapillary effect and a gravity field, when it is present, as was reflected in Eq. 24.

The flow pattern with respect to various m values is presented in Figure 9. Figure 9a shows streamlines pattern when two drops descend under the influence of gravity in the outer fluid in the absence a surface reaction and the additional effect of heat transfer ($m = 0$). This case is well known and was first presented by Haber et al.[16] The two drops move with a constant and equal velocity. Figure 9b depicts the flow in the case when heat transfer due to an exothermic surface reaction exists in the system ($m > 0$). The drops attract each other due to thermocapillary forces. Hence the migration velocity of the lower droplet decreases and that of the upper droplet increases. Figure 9c presents the unique situation when droplet interaction induced by the thermocapillary effect completely stops the motion of the lower droplet, which becomes dynamically levitating in the surrounding fluid. In this case the surface of this drop is also a stream surface in the laboratory frame of reference. In the case depicted in Figure 9d thermocapillary forces are stronger than gravity and, while the motion of the upper drop is greatly enhanced, the direction of the motion of the lower one is reversed and it now moves upward, against the sedimentation direction. This phenomenon suggests that the thermocapillary effect induced by the surface reaction can enhance or retard coalescence of two drops of equal or unequal size, which would otherwise collide under gravity, depending on whether the reaction is exothermic or endothermic, respectively.

Exothermic surface chemical reaction of a surface-active substance

In the above sections we have discussed the thermocapillary effect on the interaction of drops due to an exothermic reaction, with the sole influence on the surface tension variation stemming from local temperature gradients. When the reactant is also a surface-active substance, its local concentration affects the interfacial tension as well. In this section we consider the combined effect of the concentration of the reacting species and the temperature that results from the surface reaction. To elucidate these mutual effects they are presented in the absence of gravity though, in principle, this additional effect can be added in a similar manner to that described in the previous section.

When temperature and concentration variations are present we assume that the dependence of surface tension on these variations has the form of the bilinear expression

$$\gamma = \left(1 + \frac{\partial \gamma}{\partial T}(T-1)\right)\left(1 + \frac{\partial \gamma}{\partial C}(C-1)\right). \qquad (25)$$

Note that, since the temperature difference is always positive for an exothermic reaction and the concentration difference is negative everywhere, they have an opposing influence on the surface tension and we can expect the velocity of each drop to change direction under certain conditions. This effect is evident in Figure 10 that shows the dependence of the velocity of the drops on their separation distance and variation of several physical parameters of the problem. It can be seen that, in general, the velocity of the drops can vanish at some separation distance and thus the drops may reverse the direction of motion from attraction to repulsion and vice versa.

It is useful to compare the plots of Figure 10 to those depicted in Figure 6. While the motion demonstrated in Figure 6 reflects attraction only, in Figure 10 it is evident that transition to repulsion depends on the combination of the physical parameters. For example, while attraction was strongest at low levels of the Thiele modulus when only thermal effects were considered, when the effect is mutual to temperature and concentration gradients, attraction is evident at high moduli and the motion at low moduli becomes a repulsive one. For low values of the Thiele modulus, the diffusion rate is high relative to the reaction rate, the concentration on the surface is high and its influence on the surface tension may become stronger than the influence of the temperature. Hence, the velocity changes its sign (the drops move in reversed directions in most of the separation). For

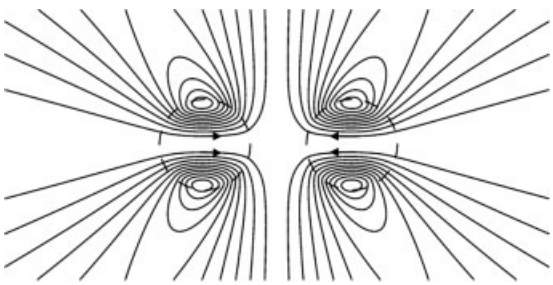

Figure 8. Flow pattern (streamlines) generated by thermocapillary driven interactions of equal drops in the absence of gravity: $d = 0.5$, $\lambda = 1$, $\kappa = 1$, $\phi^2 = 1$, $L_B = 1$.

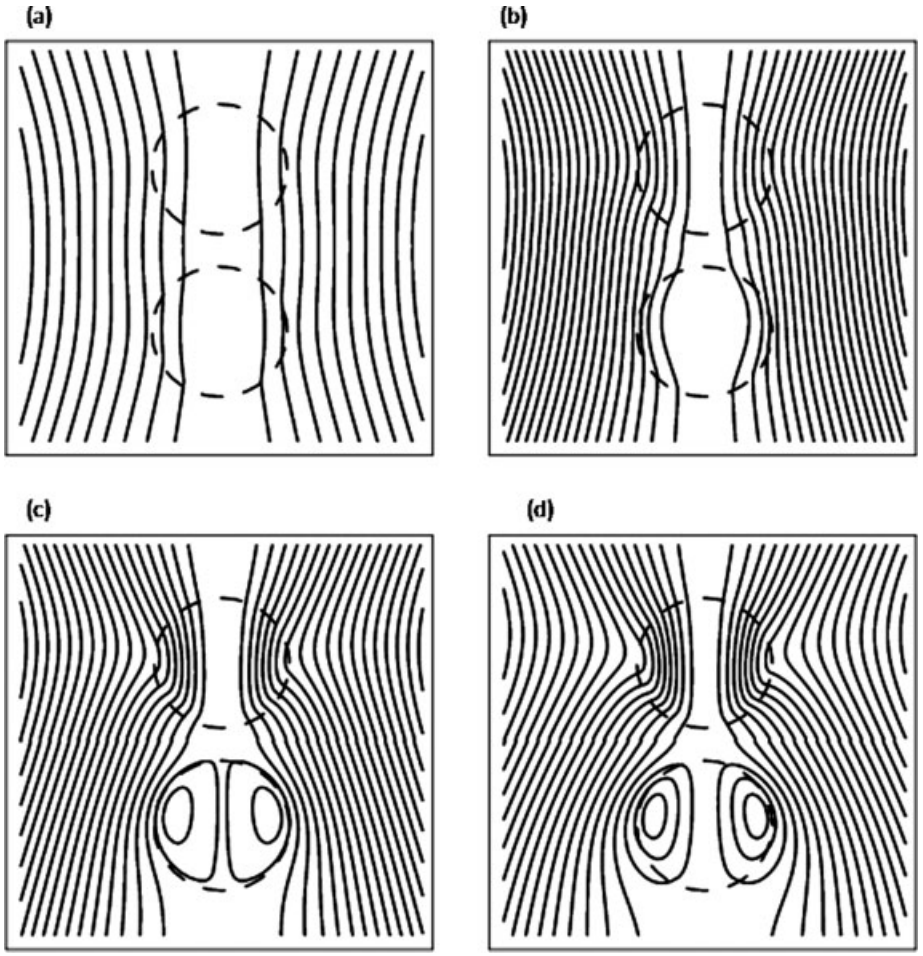

Figure 9. The influence of surface reaction on the flow in the case of two drops moving in a gravity field.

$d = 0.5$, $\lambda = 1$, $\kappa = 1$, $\phi^2 = 1$, $L_B = 1$. (a) $m = 0$ (no thermocapillary effect), $V^{(\beta_0)} = 0.381176$, $V^{(-\beta_0)} = 0.381176$; (b) $m = 20$, $V^{(\beta_0)} = 0.499126$, $V^{(-\beta_0)} = 0.263226$ (thermocapillary interaction accelerates the upper and impedes the lower one); (c) $m = 64.6255$, $V^{(-\beta_0)} = 0.499126$, $V^{(-\beta_0)} = 0$ (the lower drop levitates in the gravity field); (d) $m = 100$, $V^{(-\beta_0)} = 0.970928$, $V^{(-\beta_0)} = -0.208576$ (the lower droplet moves against gravity).

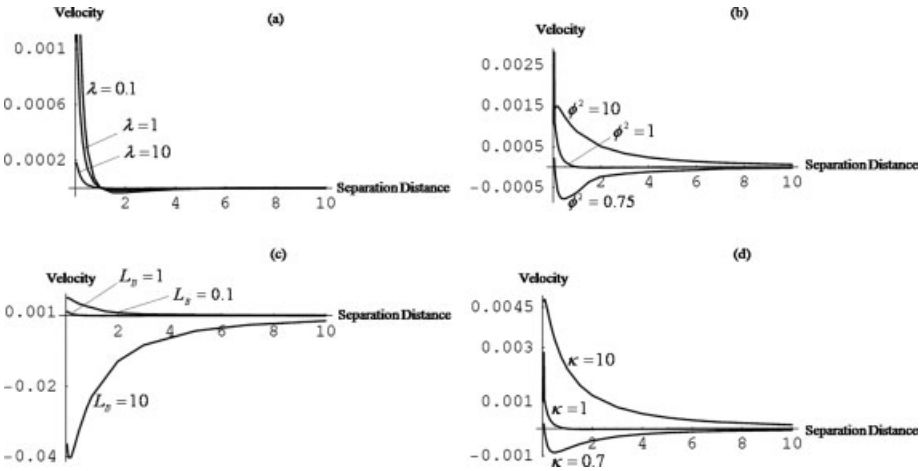

Figure 10. The influence of the separation distance on the velocity of the upper drop for various values of the different parameters of the system.

$\frac{\partial \gamma}{\partial T} = -0.5$, $\frac{\partial \gamma}{\partial C} = -0.3725$ (a) Various viscosity ratio values λ; $\phi^2 = 1$, $\kappa = 1$, $L_B = 1$; (b) various Thiele modulus (ϕ^2) values; $\kappa = 1, L_B = 1, \lambda = 1$, (c) various L_B values, $\lambda = 1$, $\phi^2 = 1$, $\kappa = 1$, (d) various thermal conductivities ratios, κ; $L_B = 1$, $\phi^2 = 1$, $\lambda = 1$.

higher values of Thiele modulus, the diffusion rate becomes smaller, the surface concentration and its gradient diminish and the influence of the temperature resumes its supremacy. At very high values of Thiele modulus ($\phi^2 \geq 10$), the influence of the temperature is always dominant and the drops move toward each other at all separation distances. Of course, the relative influence of the temperature and the concentration depends on the values of the constants $\frac{\partial \gamma}{\partial T}$ and $\frac{\partial \gamma}{\partial C}$. Similar inversion of effects is evident for the parameter L_B that reflects the ratio between the rate of release of the latent heat of reaction and the rate of heat transfer in the domains by conduction. Note also that repulsion is predicted for all examined viscosity ratios at large enough separation distances.

The plane of the parameters $\frac{\partial \gamma}{\partial C}$ and $\frac{\partial \gamma}{\partial T}$ for which the velocity of the drops is zero is presented in Figure 11 for several Thiele modulus values at given separation distance and viscosity and conductivity ratios. The straight lines reflect, of course, the choice of linear dependence of each effect (thermal and concentration) as shown in (25). Furthermore, note that for every other set of parameters, e.g. κ, L_B, λ, etc., a different set of lines is expected.

Flow pattern for the case of the combined effect of temperature and concentration on the surface tension at a considerable separation distance between levitating drops is presented in Figure 12. The separation distance between the drops is 0.7 and the net velocity of the drop is zero. Although the drop is motionless, the surface is not stationary and stagnation rings, where separation of the streamlines occurs, are evident on both side of the interface. Such patterns illustrate that there are two opposing effects on the surface and the net result depends on which effect dominates the other. In this demonstration they are in equilibrium.

In Figures 13 the transition of motion from attraction to repulsion due to the mutual effects of concentration and temperature on the surface tension is demonstrated for droplets in close proximity. In Figure 13a the drops move toward each other since the dominant influence is that of the temperature. On the other hand, in Figure 13b the influence of the concentration begins to become significant, the motion of the drops stops and the creation of stagnation points and separation of streamlines within the drops and in the outer fluid,

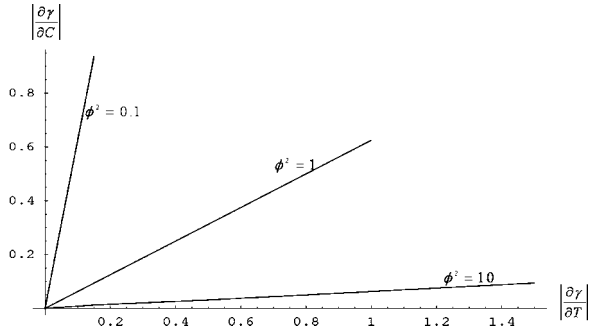

Figure 11. Phase plane of the parameters $\frac{\partial \gamma}{\partial C}$ and $\frac{\partial \gamma}{\partial T}$ in the case of motionless drops for several Thiele modulus values.

$\kappa = 1, L_B = 1, \lambda = 1, d = 1.$

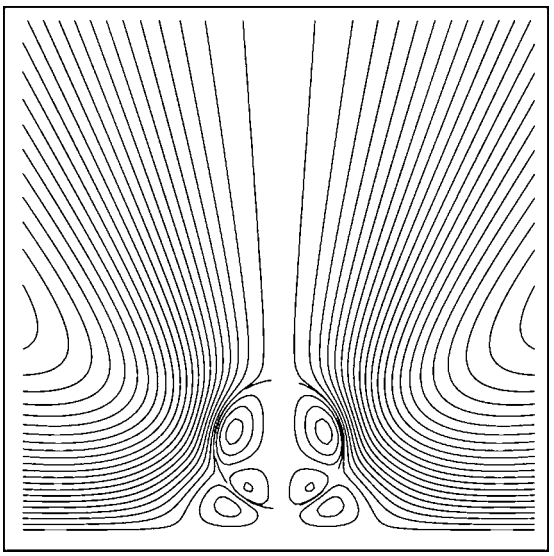

Figure 12. Flow pattern (streamlines) for the combined effect of temperature and concentration on the surface tension in the case of a motionless drop.

$d = 0.7$, $\frac{\partial \gamma}{\partial T} = -0.5$, $\frac{\partial \gamma}{\partial C} = -0.365$, $\lambda = 1$, $\kappa = 1$, $L_B = 1$, $\phi^2 = 1$.

which indicates existence of opposing forces on the interface, can be seen.

The analysis presented here does not predict whether the equilibria that are obtained as a result of the mutual effect of temperature and concentration on the surface tension are stable or not. Nevertheless, a qualitative examination of the stability of the stationary states depicted in Figure 10 is possible. Note that, in all cases shown in the figure that involve transition, the droplets attract each other when they are at very close proximity while as the separation distance increases the motion is reversed from attraction to repulsion. In all such cases it is clear that if two drops are in a motionless stationary position and a small perturbation from this separation distance occurs, the departure from equilibrium will ever increase. Hence, we can conclude that the equilibrium positions shown in this section are unstable to small perturbations.

Conclusions

In this work we studied the spontaneous motion of two drops suspended in an infinite homogeneous surfactant solution of immiscible viscous fluid when the surfactant undergoes an exothermic chemical reaction on the surface of the fluid particles. The heat of reaction results in elevation of temperature on the drops' interfaces. When another drop is present in the vicinity, the concentration and temperature in the gap region become different than those in the opposite regions. The resulting inhomogeneous distributions of concentration and temperature on the drops' interfaces result in surface tension variations, which, in turn, induce Marangoni type flow and migration of the fluid particles relative to each other.

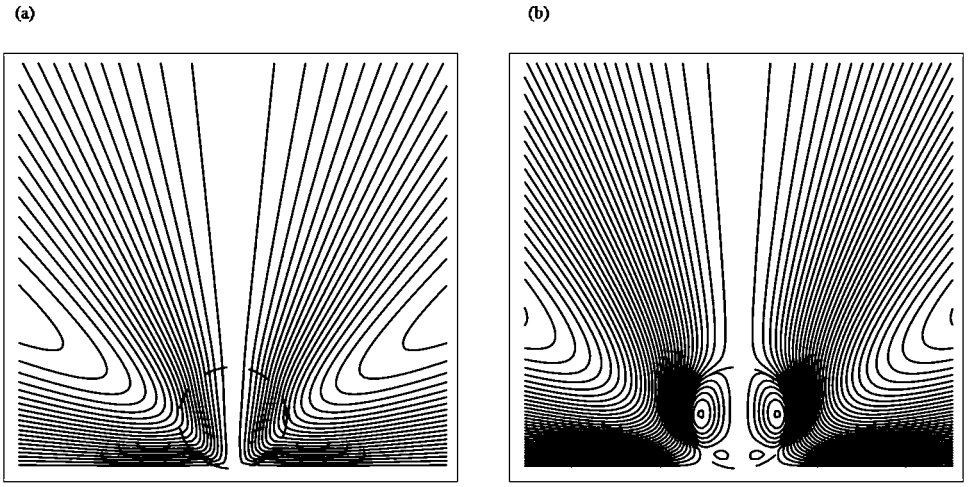

Figure 13. Flow pattern (streamlines) of the upper drop for the combined effect of temperature and concentration on the surface tension.

$\lambda = 1$, $\kappa = 1$, $L_B = 1$, $\phi^2 = 1$, $d = 0.1$. (a) $V = 0.000935121$, $\frac{\partial \gamma}{\partial T} = -0.5$, $\frac{\partial \gamma}{\partial C} = -0.3725$; (b) $V = 0$; $\frac{\partial \gamma}{\partial T} = -0.29$, $\frac{\partial \gamma}{\partial C} = -0.5$.

Three cases were considered:

• The chemical reaction, which takes place on the surface of each drop, has a significant influence on the temperature distribution, which derives the Marangoni flow, while the effect of concentration variation is neglected.

In the absence of gravity force, the drops were found to migrate towards each other at a velocity that depends on the separation distance and on the other parameters of the system.

• In the second part of the work we examined the simultaneous effect of thermocapillary force and gravity field. This section suggests that the thermocapillary interaction of two drops can strongly affect their motion in the gravity field. It was shown that when the Marangoni effect is increased, the velocity of the lower drop decreases while the velocity of the upper drop increases. At some point the drop interaction induced by the surface reaction can completely stop the gravitational migration of the lower droplet, which becomes levitating in the surrounding fluid. Further increase in the effect of the thermocapillary force results in a reversal of the direction of motion of the lower droplet, against the gravity force.

• The third part of the research considered the simultaneous effect of reactant concentration and reaction temperature on the surface tension. It is predicted that, with respect to the values of various parameters of the system, the velocity of the drops change its sign at some separation distance and the direction of the motion is reversed. At the point of zero velocity of the drops they are motionless but the surfaces are not stationary and stagnation points at which separation of the streamlines occur are observed. These dynamic stationary states, in which the thermocapillary force induced by interfacial temperature variation exactly balances the similar force created by surface concentration gradients, appear to be unstable equilibria.

Literature Cited

1. Young NO, Goldstein JS, Block MJ. The motion of gas bubbles in a vertical temperature gradient. *J Fluid Mech.* 1959;6:350–364.
2. Bratukhin YuK. Migration of a gas bubble in a non-uniformly heated liquid at small Marangoni numbers. *Inzhenerno-Fizichskii zhurnal*. 1977;32:251.
3. Subramanian RS. Thermocapillary migration of bubbles and drops. *Adv Space Res*. 1983;3:145–153.
4. Subramanian RS, Bulasubramaniam R. *The Motion of Bubbles and Drops in Reduced Gravity*. Cambridge: Cambridge University Press, 2001.
5. Levich VG. *Physicochemical Hydrodynamics*. New Jersey: Prentice hall, 1962.
6. LeVan MD, Newman J. The effect of surfactants on the terminal and interfacial velocities of a bubble or drop. *AIChE J*. 1976;22:695–701.
7. Davis RE, Acrivos A. The influence of surfactants on the creeping motion of bubbles. *Chem Eng Sci*. 1966;21:681–685.
8. Sadhal SS, Johnson RE. Stokes flow past bubbles and drops partially coated with thin films. Part 1. Stagnant cap of surfactant film-extract solution. *J Fluid Mech*. 1983;126:237–250.
9. LeVan MD. Motion of a droplet with a Newtonian interface. *J Colloid Interface Sci*. 1981;83:11–17.
10. Edwards DA, Brenner H, Wasan DT. *Interfacial Transport Processes and Rheology*. Boston: Butterworth-Heinemann, 1991.
11. Ryazantsev YuS. Thermocapillary motion of a reacting droplet in a chemically active medium. *Fluid Dyn*. 1985;20:491–495.
12. Golovin AA, Nir A, Pismen LM. Spontaneous motion of two droplets caused by mass transfer. *Ind Eng Chem Res*. 1995;34:3278–3288.
13. Golovin AA. Thermocapillary interaction between a solid particle and a gas bubble. *Int J Multiphase Flow*. 1995;21:715–719.
14. Lavrenteva OM, Leshansky AM, Berejnov V, Nir A. Spontaneous thermocapillary interaction of drops, bubbles and particles in viscous fluid driven by capillary inhomogeneities. *Ind Eng Chem Res*. 2002;41:357–366.
15. Stimson M, Jeffery GB. The motion of two spheres in a viscous fluid. *Proc R Soc*. 1926;A111:110–116.
16. Haber S, Hetsroni G, Solan A. On the low Reynolds number motion of two droplets. *Int J Multiphase Flow*. 1973;1:57–71.
17. Meyyappan M, Wilcox WR, Subramanian RS. The slow axisymmetric motion of two bubbles in a thermal gradient. *J Colloid Interface Sci*. 1983;94:243–257.
18. Meyyappan M, Subramanian RS. The thermocapillary motion of two bubbles oriented arbitrarily relative to a thermal gradient. *J Colloid Interface Sci*. 1984;97:291–294.
19. Keh HJ, Chen SH. The axisymmetric thermocapillary motion of two fluid droplets. *Int J Multiphase Flow*. 1990;16:515–527.
20. Lebedev NN. *Special Functions and Their Applications*. New Jersey: Prentice-Hall, 1965.

Appendix

The coefficients in Eq. 17 are:

$$e^n_{-1}=\frac{n}{2}\frac{\sinh\left(\left(n-\frac{1}{2}\right)\beta_0\right)}{\sinh\beta_0};\quad e^n_0=\left(\frac{1}{2}+\phi^2\right)\cosh\left(\left(n+\frac{1}{2}\right)\beta_0\right)+\left(n+\frac{1}{2}\right)\frac{\cosh\beta_0}{\sinh\beta_0}\sinh\left(\left(n+\frac{1}{2}\right)\beta_0\right);\ e^n_{+1}=\frac{n+1}{2}\frac{\sinh\left(\left(n+\frac{3}{2}\right)\beta_0\right)}{\sinh\beta_0}$$

The coefficients in Eqs. 18a,b are:

$$g^n_{-1}=\frac{1}{\sinh\beta_0}\frac{n}{2}\exp\left(-\left(n-\frac{1}{2}\right)\beta_0\right)\left(1+\kappa\frac{\sinh\left(\left(n-\frac{1}{2}\right)\beta_0\right)}{\cosh\left(\left(n-\frac{1}{2}\right)\beta_0\right)}\right)$$

$$g^n_0=\left[\frac{\cosh\beta_0}{\sinh\beta_0}\left(n+\frac{1}{2}\right)-\frac{1}{2}+\kappa\left(\frac{1}{2}+\frac{\cosh\beta_0}{\sinh\beta_0}\left(n+\frac{1}{2}\right)\frac{\sinh\left(\left(n+\frac{1}{2}\right)\beta_0\right)}{\cosh\left(\left(n+\frac{1}{2}\right)\beta_0\right)}\right)\right]\exp\left(-\left(n+\frac{1}{2}\right)\beta_0\right)$$

$$g^n_{+1}=\frac{1}{\sinh\beta_0}\frac{n+1}{2}\exp\left(-\left(n+\frac{3}{2}\right)\beta_0\right)\left(1+\kappa\frac{\sinh\left(\left(n+\frac{3}{2}\right)\beta_0\right)}{\cosh\left(\left(n+\frac{3}{2}\right)\beta_0\right)}\right)$$

$$u^n=\left[L_B\sqrt{2}+\frac{\kappa}{\sqrt{2}}+\kappa\frac{\cosh\beta_0}{\sinh\beta_0}\left(n+\frac{1}{2}\right)\sqrt{2}\frac{\sinh\left(\left(n+\frac{1}{2}\right)\beta_0\right)}{\cosh\left(\left(n+\frac{1}{2}\right)\beta_0\right)}\right]\exp\left(-\left(n+\frac{1}{2}\right)\beta_0\right)$$

$$-\frac{\kappa}{\sinh\beta_0}\exp\left(-\left(n-\frac{1}{2}\right)\beta_0\right)\left[\frac{n}{\sqrt{2}}\frac{\sinh\left(\left(n-\frac{1}{2}\right)\beta_0\right)}{\cosh\left(\left(n-\frac{1}{2}\right)\beta_0\right)}+\frac{n+1}{\sqrt{2}}\frac{\sinh\left(\left(n+\frac{3}{2}\right)\beta_0\right)}{\cosh\left(\left(n+\frac{3}{2}\right)\beta_0\right)}\exp(-2\beta_0)\right]$$

Manuscript received Apr. 27, 2007, and revision received Aug. 7, 2007.